A Synthetic Dosage Lethal Genetic Interaction Between *CKS1B* and *PLK1* Is Conserved in Yeast and Human Cancer Cells

Robert J. D. Reid,* Xing Du,† Ivana Sunjevaric,* Vinayak Rayannavar,† John Dittmar,‡,1 Eric Bryant,‡ Matthew Maurer,† and Rodney Rothstein*,2

*Department Genetics and Development and †Department of Medicine, Columbia University Medical Center, New York, New York 10032 and ‡Department of Biological Sciences, Columbia University, New York, New York 10027

ABSTRACT The *CKS1B* gene located on chromosome 1q21 is frequently amplified in breast, lung, and liver cancers. *CKS1B* codes for a conserved regulatory subunit of cyclin–CDK complexes that function at multiple stages of cell cycle progression. We used a high throughput screening protocol to mimic cancer-related overexpression in a library of *Saccharomyces cerevisiae* mutants to identify genes whose functions become essential only when *CKS1* is overexpressed, a synthetic dosage lethal (SDL) interaction. Mutations in multiple genes affecting mitotic entry and mitotic exit are highly enriched in the set of SDL interactions. The interactions between Cks1 and the mitotic entry checkpoint genes require the inhibitory activity of Swe1 on the yeast cyclin-dependent kinase (CDK), Cdc28. In addition, the SDL interactions of overexpressed *CKS1* with mutations in the mitotic exit network are suppressed by modulating expression of the CDK inhibitor Sic1. Mutation of the polo-like kinase Cdc5, which functions in both the mitotic entry and mitotic exit pathways, is lethal in combination with overexpressed *CKS1*. Therefore we investigated the effect of targeting the human Cdc5 ortholog, *PLK1*, in breast cancers with various expression levels of human *CKS1B*. Growth inhibition by *PLK1* knockdown correlates with increased *CKS1B* expression in published tumor cell data sets, and this correlation was confirmed using shRNAs against *PLK1* in tumor cell lines. In addition, we overexpressed *CKS1B* in multiple cell lines and found increased sensitivity to *PLK1* knockdown and PLK1 drug inhibition. Finally, combined inhibition of WEE1 and PLK1 results in less apoptosis than predicted based on an additive model of the individual inhibitors, showing an epistatic interaction and confirming a prediction of the yeast data. Thus, identification of a yeast SDL interaction uncovers conserved genetic interactions that can affect human cancer cell viability.

KEYWORDS CKS1; cyclin-dependent kinase; polo-like kinase; synthetic dosage lethal

THE *CKS1B* gene is frequently overexpressed in breast, lung, and liver cancers due to amplification of chromosome 1q21 (Chang *et al.* 2002; The Cancer Genome Atlas Network 2012). *CKS1B* is a highly conserved member of the *CKS1/suc1* gene family that plays important roles in cell cycle control through interactions with cyclin-dependent kinase (CDK) and SCF complexes (Figure 1A) (Bourne *et al.* 1996, 2000; Ganoth *et al.* 2001; Spruck *et al.* 2001). Increased expression of *CKS1B* is negatively associated with survival in both breast cancer and hepatocellular carcinoma (Slotky *et al.* 2005; Huang *et al.* 2010). It is important to note that gene amplification, *per se*, does not indicate whether *CKS1B* is a "driver" or "passenger" gene in oncogenesis (Santarius *et al.* 2010; Vogelstein *et al.* 2013), and multiple genes are included in copy number amplification of the 1Q21 region (Chen *et al.* 2010).

Cks1 was first identified in fission and budding yeasts as *suc1* and *CKS1*, respectively, essential genes that dosage suppress the G1 phase cell cycle arrest of specific temperature-sensitive CDK mutations (Hayles *et al.* 1986b; Hadwiger *et al.* 1989). The Cks1 protein in both organisms was also shown to associate with the CDK (Hayles *et al.* 1986a; Brizuela *et al.* 1987; Hadwiger *et al.* 1989). Further genetic analyses revealed a role for Cks1 to promote both the G1–S and

doi: 10.1534/genetics.116.190231
Manuscript received April 7, 2016; accepted for publication August 11, 2016; published Early Online August 23, 2016.
Available freely online through the author-supported open access option.
Supplemental material is available online at www.genetics.org/lookup/suppl/doi:10.1534/genetics.116.190231/-/DC1.
[1]Present address: Teladoc, Inc., 2 Manhattanville Rd., Purchase, NY 10577.
[2]Corresponding author: Columbia University Medical Center, Department of Genetics & Development, 701 W. 168th St., HHSC 1608, New York, NY 10032-2704. E-mail: rothstein@columbia.edu

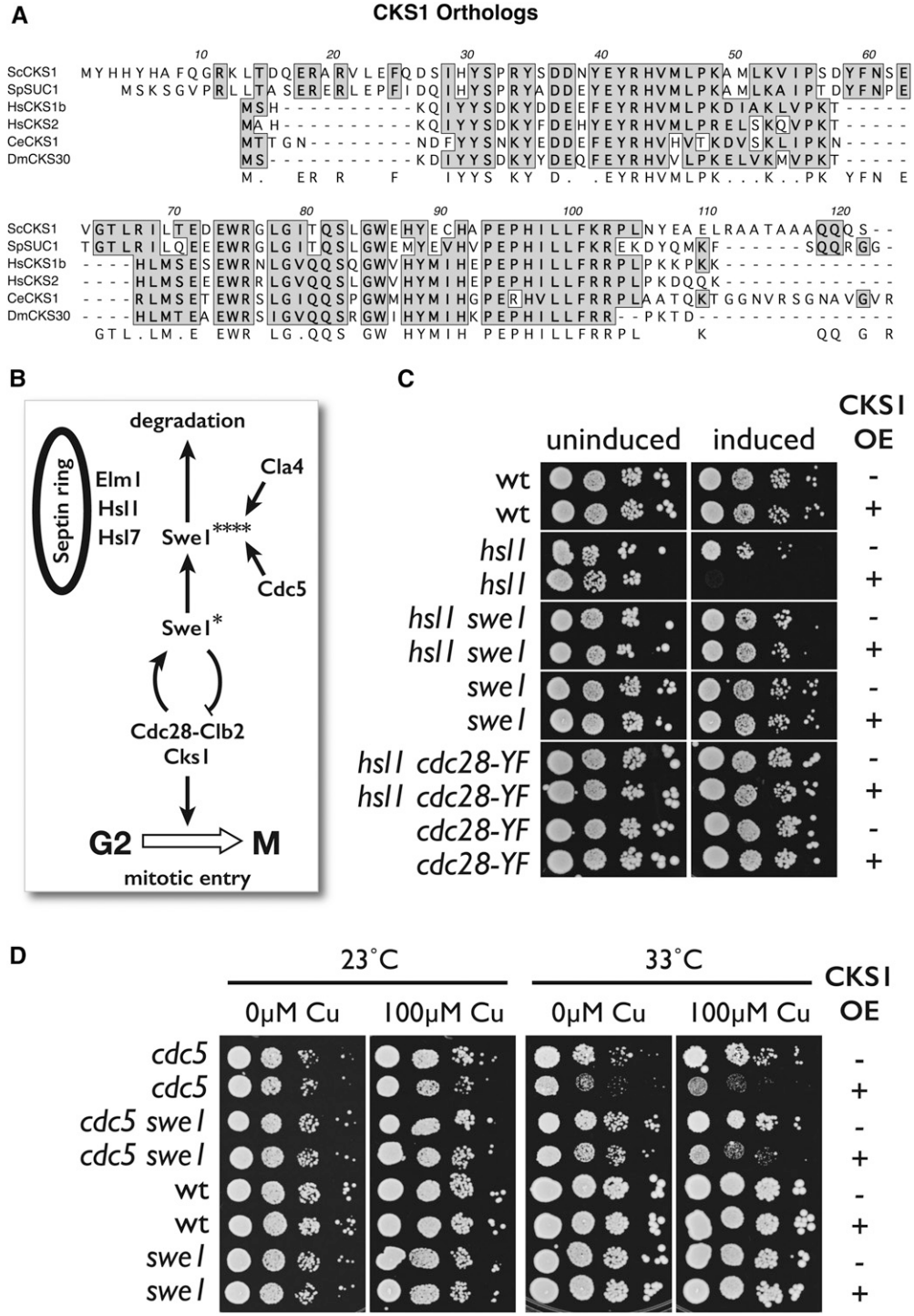

Figure 1 Sensitivity of morphogenesis checkpoint genes to *CKS1* expression. (A) Multiple sequence alignment of Cks1 proteins from *S. cerevisiae* (ScCKS1), *S. pombe* (SpCKS1), human (HsCKS1b and HsCKS2), *Caenorhabditis elegans* (CeCKS1), and *Drosophila melanogaster* (DmCKS30) using the ClustalW version 1.83. (B) Model of Swe1 function in mitotic entry. Entry into mitosis is depicted at the bottom by the large open arrow. The CDK complex, consisting of Cdc28, Clb2, and Cks1, regulates entry into mitosis and also provides initial phosphorylations on Swe1 (arrow and *). Phospho-Swe1 is an active inhibitor of the CDK complex (inhibition arrow). Phospho-Swe1 is localized to the septin ring (oval) through its interaction with the Elm1–Hsl1–Hsl7 complex. Cdc5 and Cla4 multiply phosphorylate Swe1 (****), leading to its degradation. (C) The *CKS1* expression plasmid (pWJ2040 indicated by +), or an empty vector control (pWJ1781 indicated by −) were transformed into wild-type (W9100-17D), *hsl1* (W10096-7C), *hsl1 swe1* (W10096-2D), or *swe1* (W11020-4A) strains. Cultures were grown overnight, equalized to the same OD_{600}, 10-fold serially diluted, then 5-μl drops were spotted onto plates with glucose to repress, or galactose to induce, *CKS1* expression. (D) Plasmids expressing *CKS1* from a copper-inducible promoter (pWJ1785 indicated by +) or an empty vector control (pWJ1512 indicated by −) were transformed into *cdc5-1* (W11066-6A), *cdc5-1 swe1* (W11066-6A), wild-type and *swe1* strains, grown as above, and spotted onto plates with or without 100 μM $CuSO_4$ at 23° and 33°.

G2–M cell cycle transitions (Tang and Reed 1993). In addition, cloning of two human genes, *CKS1B* and *CKS2*, both of which complement yeast *CKS1* deletion mutants, showed that *CKS1* orthologs exist in human cells (Draetta *et al.* 1987; Richardson *et al.* 1990). Thus, Cks1 functions at multiple points during the cell cycle and is highly conserved from fungi to humans.

A conserved role for Cks1 in mitosis was also demonstrated by depleting Cks1 from *Xenopus* oocyte extracts, which show a block at the G2–M transition due to accumulation of an inhibitory phosphorylation on the CDK (Patra and Dunphy 1996). Paradoxically, addition of excess Cks1 to these extracts also inhibits the activity of the *Xenopus* CDK and delays mitosis by inhibiting dephosphorylation of the regulatory tyrosine residue (Dunphy and Newport 1989; Patra and Dunphy 1996). Furthermore, excess Cks1 in these extracts results in phosphorylation of the CDK regulators Cdc25, Myt1, and Wee1. The net result of these modifications activates the CDK

dephosphorylation activity of Cdc25, and also inactivates Myt1 and Wee1 so that they no longer inhibit the CDK. Together, these regulatory events promote entry into mitosis (Patra *et al.* 1999). Thus, both increased and decreased levels of Cks1 can affect mitotic progression, underscoring the complexity of these regulatory circuits.

Cks1 proteins bind to cyclin-dependent kinase complexes, but the functional consequences of binding vary. Cks1 is required for G1 cyclin–CDK kinase activity in budding yeast, but not for B-type cyclin–CDK activity (Reynard *et al.* 2000). A crystal structure of human CKS1B in complex with CDK2 identified the CKS1B–CDK interface as well as a pocket in CKS1 that can coordinate binding of a phosphate residue (Bourne *et al.* 1996, 2000). Moreover, recent work shows that CDK–CKS1 complexes specifically bind phosphothreonine residues, suggesting a model in which CKS1 helps target CDK activity to previously phosphorylated CDK substrates to promote processive modification and regulation of those proteins (McGrath *et al.* 2013). Thus Cks1 acts as a specificity factor for the CDK. One example of this specificity is that Cks1 is required for the CDK-dependent phosphorylation of the CDK inhibitor Sic1, leading to its SCF-dependent destruction, which allows entry into S phase (Kõivomägi *et al.* 2011).

Finally, Cks1 also has important interactions with the proteasome. In mammalian cells, CKS1B targets SCF–SKP2 ubiquitin ligase to the CDK inhibitor $p27^{KIP}$/CDKN1B to promote its degradation and allow entry into S phase (Ganoth *et al.* 2001; Spruck *et al.* 2001; Barberis *et al.* 2005). Interactions of Cks1 with the proteasome are also conserved. In yeast, Cks1 affects transcription of CDC20—which codes for an M phase-specific component of the anaphase-promoting complex (APC)—by periodic recruitment of the proteasome to the CDC20 promoter region (Morris *et al.* 2003).

Although aspects of *CKS1* function are becoming clearer, the effect of increased CKS1B expression in multiple cancers is unknown. Here we take advantage of the high conservation of Cks1 function in the yeast *Saccharomyces cerevisiae* to perform a genome-wide search for mutations that are sensitive to *CKS1* overexpression, a genetic interaction termed synthetic dosage lethality (SDL) (Measday and Hieter 2002). In addition, these SDL interactions give us insight into the pathways affected by *CKS1* overexpression. Interestingly, multiple mutations affecting mitotic entry and mitotic exit were identified as SDL with *CKS1* overexpression, including the polo-like kinase Cdc5, an ortholog of human PLK1. Finally, experiments in cancer cells show that this SDL is conserved, as overexpression of *CKS1B* results in increased sensitivity to *PLK1* inhibition.

Materials and Methods

Yeast strains and methods

Yeast gene disruption strain libraries in the BY4741 or BY4742 strain backgrounds for high throughput SDL screens were obtained from Thermo Fisher Scientific (Waltham, MA) (Winzeler *et al.* 1999). The yeast library of temperature-sensitive alleles for essential genes in the BY4741 background was a kind gift of Brenda Andrews (University of Toronto). Standard yeast growth media and culture techniques were used throughout this work (Sherman *et al.* 1986). Selective ploidy ablation (SPA) was used for high throughput transfer of expression plasmids into yeast strain libraries for SDL screens as previously described (León Ortiz *et al.* 2011; Reid *et al.* 2011). Colony growth was measured from scanned plate images using ScreenMill software as previously described (Dittmar *et al.* 2010). Colony growth data processed via ScreenMill is provided in the Supplemental Material, File S1). Replica pinning for the SPA procedure was accomplished using a Singer RoToR HDA robot (Singer Instruments, Somerset, UK). Validation of individual SDL interactions and analysis of suppressor mutations was carried out in the W303 genetic background (Thomas and Rothstein 1989). Disruptions of nonessential genes were PCR amplified from the gene disruption library strains to produce a DNA fragment containing the KanMX selectable marker plus 300–400 bp of flanking homologous sequence, then transformed into stain W9100-17D (Herrero and Thorpe 2016). The resulting gene disruption strains were combined with additional mutants by standard genetic crosses. Mutant alleles from the essential library were transferred into the W303 background by three or more backcrosses. G418 and clonNAT were purchased from MediaTech and Werner Bioagents, respectively. LiOAc transformations were performed as described (Schiestl and Gietz 1989).

Yeast plasmids

To construct pWJ1781, plasmid pWJ1512 (Reid *et al.* 2011) was digested with restriction enzymes *Bam*HI and *Spe*I and the 6.4-kbp fragment was isolated. The pGAL1 promoter from pWJ1047 (Wagner *et al.* 2006) was PCR amplified as a 810-bp fragment using primers JD-Gal_UP (5′-CACCGCGGTGGCGGCCGGCCGCTCTCGCG ACACGAGGCCCTTTCGTCTTC-3′) and ADH1term-rev (5′-CAACCTTGATTGGAGACTTG-3′). The purified DNA fragments were recombined by transformation into yeast strain W9100-17D. To construct a copper-inducible *CKS1* expression plasmid, pWJ1785, the *CKS1* open reading frame (ORF) was PCR amplified from yeast strain W9100-17D using primers CKS1-A (5′-GGAATTCCAGCTGACCACCCTATGTAC CATCACTATCACGCC-3′) and CKS1-B (5′-GATCCCCGG GAATTGCCATGCAGTAATTAGAGTATATCAAAGCTAG-3′). Purified DNA was recombined with pWJ1512 plasmid DNA linearized by *Hpa*I restriction digest. A galactose-inducible *CKS1* expression plasmid, pWJ2040, was constructed from the same *CKS1* PCR fragment, but recombined into plasmid pWJ1781 linearized at the *Hpa*I restriction site. A high copy number *SIC1* plasmid was constructed as follows. First, the cloning region of plasmid pWJ1250 (Alvaro *et al.* 2007) was PCR amplified with primers 304-F (5′-TAAGTTGGGTAACGC CAGGGT-3′) and 304-R (5′-CGGCTCCTATGTTGTGTGGAAT-3′),

Table 1 Genes identified in SDL screens by *CKS1* overexpression

Function	Gene name
Morphogenesis checkpoint	*HSL1*† *HSL7*† *ELM1*†
Septins	*CDC10*† *CDC11 CDC12*† *CDC3*
PAK kinase	*CLA4*†
Polo-like kinase	*CDC5*†
Mitotic exit network	*LTE1*† *CDC15*† *DBF22*† *CDC14*†
Anaphase promoting complex	*CDH1*†
S phase progression	*DPB11*†
Kinetochore	*DAM1 ASK1 NDC80 SPC24*† *SPC25*† *DSN1 NNF1 NSL1 OKP1 AME1 CBF2 MIF2*†
Cell polarization	*VRP1 ACT1 LAS17 MYO2*
CDK complex	*CDC28*
Others	*ERG11 LUC7 NOP2 RPC40 RPT6 ANP1 RSP5 SEC26 SPC110 SWC4 SWD2 MRPS5*

† Mutant allele transferred to W303 background for further analysis.

then recombined into the 2μ plasmid pRS426 (Christianson *et al.* 1992) to make pWJ2146. Next, *SIC1* DNA was PCR amplified from strain W9100-17D with primers C-SIC1 (5′-ccgctgctaggcgcgccgtgGCTTCACAGCATGGTTGTAAAGAGCG TTCTA-3′) and D-SIC1 (gcagggatgcggccgctgacCCCCTAACT CGCTTTGACGAAATACTAC), then transformed into pWJ2146 linearized with *Hpa*I to make plasmid pWJ2147. All plasmid constructs were verified by sequencing (GENEWIZ, South Plainfield, NJ).

Mutual exclusion analysis

Breast cancer cohort RNA microarray expression data were obtained from the published 2012 breast cancer data set (The Cancer Genome Atlas Network 2012). Pan cancer analysis was performed using RNA seq V2 data (release July 15, 2014) obtained from the Broad Institute Firehose (http://gdac.broadinstitute.org/).

Gene Activity Ranking Profile data analysis

Gene Activity Ranking Profile (GARP) data for the breast cancer cells described in Marcotte *et al.* (2012) were acquired from the Donnelly–Princess Margaret Screening Centre website (http://dpsc.ccbr.utoronto.ca/cancer/) at the University of Toronto. A messenger RNA (mRNA) expression data set GSE36133 was obtained from the cancer cell line encyclopedia (http://www.broadinstitute.org/ccle) (Barretina *et al.* 2012).

Cell lines and antibodies

MCF7, MDA-MB-157, BT-20, MDA-MB-453, and HS578T cells were obtained from the American Type Culture Collection (ATCC) and cultured in DMEM media and 10% FBS. HCC-1143, HCC-1806, HCC-1569, and HCC-70 were obtained from ATCC and cultured in RPMI-1640 media and 10% FBS. Human mammary epithelial cell (hMEC)–human telomerase reverse transcriptase (hTERT) cells were cultured in DMEM/F12 media and 5% horse serum supplemented with EGF (20 ng/ml), hydrocortisone (500 ng/ml), insulin (10 μg/ml), and cholera toxin (100 ng/ml). All cells were cultured with 1% penicillin/streptomycin at 37° with 5% CO_2. PLK1 antibody was obtained from Cell Signaling Technology (Danvers, MA) and CKS1B antibody was obtained from Invitrogen (Carlsbad, CA).

Protein blotting, competition assay, and apoptosis assays

Cells were lysed with 2× Laemmli buffer. Equal amount of total proteins were separated by electrophoresis and transferred to polyvinylidene fluoride membranes. Membranes were incubated with primary antibodies followed by secondary antibodies and then developed with an enhanced chemiluminescence detection kit according to the manufacturer's instructions (Thermo Fisher Scientific).

Cell lines were transduced with TRIPZ-based shPLK1 lentivirus with doxycycline-inducible TurboRFP fluorescent reporter (GE Healthcare Dharmacon, Lafayette, CO, RHS4696-200773058) and selected with varying concentration of puromycin, based on individual killing curves. To check the knockdown of PLK1, puromycin-resistant shPLK1 cells were induced with doxycycline 1 μg/ml for 3 days. Cell lysates were prepared, proteins were size resolved by SDS-PAGE, and then transferred to membranes for protein blotting of PLK1.

To monitor the effects of PLK1 knockdown on cell growth with competition assay, puromycin-resistant shPLK1 cells were mixed 1:1 with noninfected parent cells and knockdown of PLK1 was induced by doxycycline. The percentages of RFP^+ cells were analyzed with flow cytometry on day 2 and day 5 after doxycycline induction. The day 2 RFP^+ cells were set as 100% and decrease of RFP^+ cells on day 5 was expressed as growth inhibition.

HS578T cells with the doxycycline-inducible shPLK1 lentivirus were further transduced with a CKS1B ORF expressing lentivirus with a GFP reporter (GE Healthcare Dharmacon, OHS5897-202616021) or an empty GFP-expressing lentivirus as a negative control. GFP^+ cells were sorted with the FacsAria Cell Sorter (Beckton Dickinson, San Jose, CA). The GFP-expressing cells were mixed with an equal number of parent HS578T cells, and PLK1 short hairpin RNA (shRNA) was induced with doxycycline. The results from the competition

assay were measured on day 2 and day 5 for RFP/GFP$^+$ cells. To measure the apoptotic cells induced by *PLK1* knockdown or inhibition, the cells were treated with doxycycline or PLK1 inhibitor Volasertib (Selleckchem, Houston, TX) for 3 days. Cells were then trypsinized and stained with APC Annexin V (Becton Dickinson). Apoptic cells are defined as APC Annexin V$^+$.

To explore the effect of combined PLK1 and Wee1 inhibition, cells were treated with Volasertib and/or Wee1 inhibitor MK-1775 (Selleckchem) for 3 days. Both floating cells and adherent cells were collected and stained with APC Annexin V (Becton Dickinson). Background levels of apoptotic cells from nontreatment wells were deducted from each treatment group. The Bliss independence model was used to determine synergism or antagonism (Bliss 1939). In an additive model, the combined effects of drug A and B = $A\% + B\% - A\% \times B\%$, where $A\%$ = percent growth inhibition from compound A, and $B\%$ = percent growth inhibition from compound B. Inhibition greater than the additive model indicates a synergistic effect of two drugs. Inhibition less than the additive model indicates antagonism.

Data availability

All data from genome-wide screens are included in File S1.

Results

Identification of mutations sensitive to CKS1 overexpression

To identify SDL interactions with overexpressed *CKS1*, we carried out a high throughput screen of yeast gene disruption libraries. A low copy number plasmid with *CKS1* expressed from the galactose-inducible *GAL1* promoter was transferred into ~9600 gene disruption strains in the *MAT***a** and *MAT*α libraries by SPA (Winzeler *et al.* 1999; Reid *et al.* 2011). Four replicates of each library strain were tested in a 1536-colony array. The effect of *CKS1* expression on growth in each strain was determined by comparison of colony sizes in cells containing the *CKS1* expression vector in parallel to colonies with the empty vector controls (Dittmar *et al.* 2010). Affected sets for each screen were determined after rank ordering screen results by growth ratio and then using the CLIK algorithm to define the bounds of the highly interacting genes at the top of the rank order (Dittmar *et al.* 2013). CLIK analysis identified sets of 74 and 70 genes for the *MAT***a** and *MAT*α libraries, respectively; however the interaction density in these sets is low, suggesting few true positives (Figure S1A). Because of this result, we focused on the 10 genes that are common to the CLIK groups from both screens for validation and further analysis (Table S1). Eight of the 10 genes function in the establishment of cell polarity or cell cycle progression.

We next expressed *CKS1* in a yeast strain library containing temperature-sensitive alleles of essential genes using the SPA procedure (Li *et al.* 2011). In this case, the final SPA selection plates were printed in quadruplicate and grown at 23°, 27°, 30°, and 33° to test the effect of *CKS1* expression at varying temperatures. Two complete screens were performed and strains showing a twofold or greater growth difference between control and *CKS1* expression in both screens at the same temperature conditions were identified (Table S2).

The accumulated results from SDL screens in all mutant libraries define 44 genes that are grouped by function and listed in Table 1. Many of the genes isolated in the *CKS1* screens affect progression through mitosis. The genes affecting mitotic progression can be further subdivided into genes affecting mitotic entry and genes affecting mitotic exit. Mutant alleles for 15 of the genes in Table 1 affecting different aspects of mitotic progression (marked with *) were transferred into the W303 strain background for additional experiments (see *Materials and Methods*) (Thomas and Rothstein 1989). Of these, only the *cdc10-4* mutant failed to recapitulate the SDL interaction with *CKS1* overexpression in W303.

The CKS1 SDL interaction with mitotic entry mutants is dependent on Swe1

To understand the mechanism of sensitivity of mutations affecting mitotic entry to *CKS1* overexpression, we examined genetic interactions in the morphogenesis checkpoint pathway. This pathway ensures that cells enter mitosis only after bud emergence (Figure 1B and reviewed in Howell and Lew 2012). Mitotic entry is delayed by a Swe1-dependent phosphorylation of Cdc28 on a conserved tyrosine residue (Y19) (Booher *et al.* 1993). Swe1 is initially phosphorylated by the CDK, which serves to activate Swe1 inhibitory function while also marking it for degradation (Sia *et al.* 1998; Harvey and Kellogg 2003). Phosphorylated Swe1 is localized to the septin ring through its interaction with the Elm1–Hsl1–Hsl7 complex, where it is multiply phosphorylated by kinases including Cdc5 and Cla4, ubiquitylated by the SCF complex, and then degraded (Sia *et al.* 1998; McMillan *et al.* 1999; Sakchaisri *et al.* 2004). Defects in septin ring assembly hinder the localization of Swe1 to the bud neck, which inhibits Swe1 degradation, resulting in mitotic delay (Longtine *et al.* 2000; Cid *et al.* 2001). To test whether the CKS1 SDL interaction with the Elm1–Hsl1–Hsl7 complex required the function of Swe1, each mutant was combined with a *swe1* null mutation and measured for growth upon induction of *CKS1* expression (Figure 1 and Figure S2). Growth inhibition of *hsl1* (Figure 1C), *hsl7*, or *elm1* (Figure S2A) due to *CKS1* overexpression is completely suppressed by deletion of *swe1*. To test whether the effect of *CKS1* overexpression on Swe1 functions through direct regulation of the CDK as opposed to other targets of the Swe1 kinase, a nonphosphorylatable *CDC28* allele (tyrosine 19 to phenylalanine, *cdc28-Y19F*) was constructed (see *Materials and Methods*). The *cdc28-Y19F* allele combined with *hsl1* and *elm1* also results in complete suppression of *CKS1* sensitivity (Figure 1C and Figure S2B). Therefore the effect of *CKS1* overexpression in *elm1*, *hsl1*, and *hsl7* mutants is mediated by the activity of Swe1 on the CDK complex.

Two additional kinases, Cla4 and Cdc5, both localize to the bud neck and can phosphorylate Swe1 *in vitro* (Sakchaisri

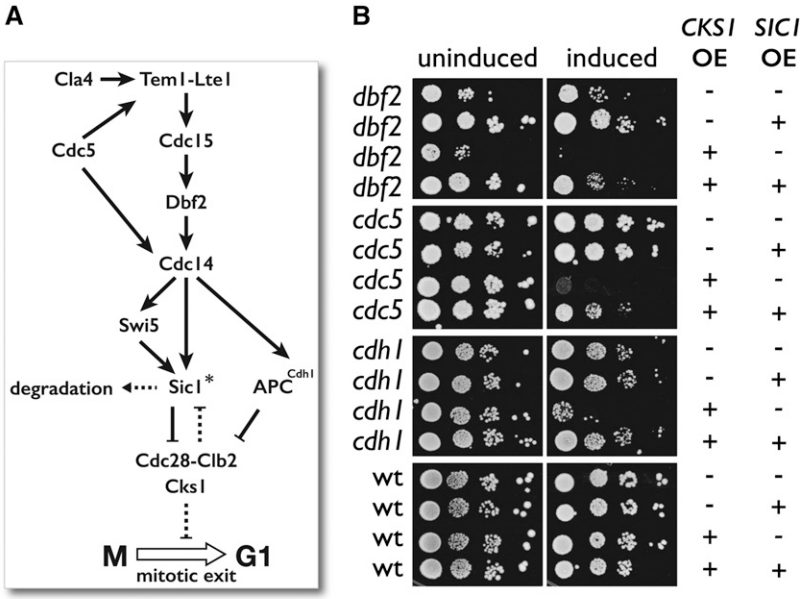

Figure 2 Sensitivity of mitotic exit network mutants to *CKS1* expression. (A) Model of Sic1 function during mitotic exit. CDK activity driven by B-type cylins inhibits entry into G1 phase. As described in the text, the mitotic exit network promotes the M–G1 transition via a kinase cascade leading to activation of the Cdc14 phosphatase, which stabilizes Sic1, enhancing its CDK inhibitory function. Dashed lines indicate a model for CKS1 overexpression where increased CKS1 promotes Sic1 targeting and phosphorylation by the CDK complex, leading to degradation of Sic1 and inhibition of mitotic exit. (B) *dfb2* (W11090-5D), *cdc5-1* (W11099-16B), *cdh1* (W11038-4B), and wild-type (W9100-17D) strains were transformed with the following plasmids: The *CKS1* expression plasmid (pWJ2040, + under *CKS1* OE column) or vector control (pWJ1781, − under *CKS1* OE column) and a high copy plasmid constitutively expressing *SIC1* (pWJ2147, + under *SIC1* OE column) or a vector control (pRS426, − under *SIC1* OE column). Strains were grown and spotted onto selection media as in Figure 1. Uninduced indicates growth on glucose-containing medium where *CKS1* expression is repressed, and induced indicates galactose-containing medium for induction of *CKS1* expression.

et al. 2004). Furthermore, Swe1 accumulates as multiply modified species in cells lacking Cdc5 (Sakchaisri *et al.* 2004), indicating that polo-like kinase activity is necessary for Swe1 degradation. We therefore tested whether sensitivity to *CKS1* overexpression in *cdc5* and *cla4* mutants was also a function of Swe1 activity. For these studies, we used the *CUP1* promoter (Butt *et al.* 1984; Gorman *et al.* 1986), as it is weaker than the galactose promoter and allows greater sensitivity to suppression levels. As seen in Figure 1D, growth arrest is observed at the semipermissive temperature (33°) in *cdc5-1* mutants even under conditions of low basal *CUP1* promoter expression of *CKS1* (0 Cu^{2+} addition). Deletion of *swe1* suppresses this growth arrest, albeit incompletely, for both the basal and induced conditions (Figure 1D). Deletion of *swe1* did not suppress the *CKS1* SDL with a *cla4* mutant (Figure S2C) and did not suppress the effect of the galactose-induced *CKS1* interaction in a *cdc5* strain (Figure S2D). The incomplete suppression of the *CKS1* SDL by *swe1* suggests that the Cdc5 and Cla4 kinases participate in other pathways in the cell that are affected by *CKS1* overexpression. Indeed, these kinases function in multiple pathways throughout mitosis, including the mitotic exit network. Since several mitotic exit network mutants were identified in the screens (Table 1), we next examined their role in *CKS1* sensitivity.

The CKS1 SDL interaction with mitotic exit mutants is suppressed by SIC1 overexpression

The mitotic exit network is a signal cascade initiated in postanaphase cells, which leads to inactivation of the CDK complex and dephosphorylation of mitotic CDK targets. As shown in Figure 2A, the mitotic exit network, composed of Tem1-Lte1, Cdc15, Dbf2, and Cdc14, promotes the M–G1 transition by Cdc14-dependent induction of Swi5, which induces expression of the CDK inhibitor Sic1, thereby inhibiting CDK activity leading to mitotic exit (Toyn *et al.* 1997; Bardin and Amon 2001). Cdc14 also dephosphorylates and stabilizes Sic1, enhancing its CDK inhibitory function. Additionally, Cdc14 activates the APC via Cdh1, promoting destruction of B-type cyclins to ensure mitotic exit. The Cla4 and Cdc5 kinases both have roles in regulating the mitotic exit network via control of the spindle position checkpoint (arrows toward Tem1 in Figure 2A). Additionally, Cdc5 directly influences release of the Cdc14 phosphatase from the nucleolus (Visintin *et al.* 2003; Piatti *et al.* 2006). Several of these mutations affecting the mitotic exit network can be suppressed by increased expression of *SIC1* (Jaspersen *et al.* 1998). Since Cks1 plays a positive role in the phosphorylation and degradation of Sic1 during the G1–S phase transition (McGrath *et al.* 2013), we tested whether increased *SIC1* expression would suppress the effect of *CKS1* overexpression in the mitotic exit network mutants. *SIC1* expression from a high copy plasmid suppresses the *CKS1*-induced arrest of *dbf2* and *cdc15* (Figure 2B and Figure S3C). Similarly, mutations in *cdh1*, a component of the APC, arrest growth in response to *CKS1* overexpression. This growth arrest is also suppressed by increased expression of *SIC1* (Figure 2B). We also find that increased *SIC1* expression suppresses the effect of *CKS1* overexpression in *cdc5* and *cla4* mutants (Figure 2B and Figure S3B).

Most of our results point to the regulation of mitotic entry and mitotic exit by Swe1 and Sic1, respectively, being genetically separable. For example, the *CKS1-cla4* SDL, which is suppressed by *SIC1* overexpression (Figure S3B), is not suppressed by *SWE1* deletion (Figure S2C). Likewise the *CKS1-hsl1* SDL is not suppressed by increased *SIC1* expression (Figure S4B), but is suppressed by *SWE1* deletion (Figure 1C). However, it is important to note that Cdc5 affects both pathways (Sia *et al.* 1998; Visintin *et al.* 1998; McMillan *et al.* 1999; Piatti *et al.* 2006). Indeed, we find that the *CKS1*-induced arrest in a *cdc5-1* mutant is partially suppressed by

deletion of *swe1* (mitotic entry) and also partially suppressed by increased expression of *SIC1* (mitotic exit) (Figure 1D and Figure 2B).

The CKS1-PLK1 SDL is conserved in cancer cell lines

Since the polo-like kinase Cdc5 is common to the mitotic entry and mitotic exit pathways when *CKS1* is overexpressed, we turned our attention to PLK1, the human ortholog of yeast Cdc5. PLK1 regulates many aspects of mitosis, having conserved roles in the G2–M transition, APC regulation, and cytokinesis (reviewed in Zitouni *et al.* 2014), and is an established antimitotic target in cancer therapy (Degenhardt and Lampkin 2010). We analyzed breast cancer gene expression data from The Cancer Genome Atlas to determine whether there is a relationship between *CKS1B* and *PLK1* in human cells (Cerami *et al.* 2012; The Cancer Genome Atlas Network 2012). Mutual exclusion of genetic alterations in cancer sequencing data can be used to predict synthetic lethal relationships between two genes (Unni *et al.* 2015). *CKS1B* mRNA expression is increased (z-score ≥ 2) in 90 (17%) of the samples in the published data set. *PLK1* mRNA expression was decreased (z-score < -1) in 78 (15%) of the tumor samples. These expression patterns did not co-occur (0 tumors with both) and are considered mutually exclusive (hypergeometric P-value $= 1.2 \times 10^{-7}$). This mutual exclusion is not restricted to breast cancer. In an analysis of 1080 samples across all cancer cohorts, *CKS1B* expression is increased in 784 samples and *PLK1* expression is decreased in 303 samples (See *Materials and Methods*). The co-occurrence of these conditions exists in only seven samples (hypergeometric P-value $<10^{-24}$). Thus, mutual exclusion of increased *CKS1B* and decreased *PLK1* expression is consistent with a conserved SDL interaction.

We next analyzed a data set of shRNA knockdowns covering ~16,000 human genes in a set of 28 breast cancer cell lines for further evidence of a genetic interaction between *CKS1B* and *PLK1* (Marcotte *et al.* 2012). In that study, the effect of shRNA knockdown on cell growth at multiple time points after shRNA induction was used to derive an overall effect on viability called a GARP score. *CKS1B* expression status for each of the cell lines used in that study was acquired from microarray data available from the Cancer Cell Line Encyclopedia (Barretina *et al.* 2012). Correlations were calculated between *CKS1B* expression and GARP scores for the 16,000 genes in the study (see *Materials and Methods*). *CKS1B* expression negatively correlates with the *PLK1* GARP score ($r = -0.554$, $r^2 = 0.31$) and is in the top 0.8th percentile of all correlations examined with CKS1B (117 of 16,028), suggesting that increased *CKS1B* expression sensitizes cells to decreases in *PLK1* expression, consistent with the *CKS1* SDL interaction with *cdc5* in yeast cells (Figure 3A).

Based on the evidence above, we next measured the effect of *PLK1* knockdown in eight of the breast cancer cell lines used in the GARP study along with breast cancer cell line HCC-1569. The nine cell lines, which have varied levels of *CKS1B* expression, were transduced with a doxycycline-inducible PLK1 shRNA lentivirus. Immunoblots were used to assess the relative amount of PLK1 and CKS1B in each cell line (Figure 3B). CKS1B protein levels broadly agreed with mRNA expression levels from the Cancer Cell Line Encyclopedia

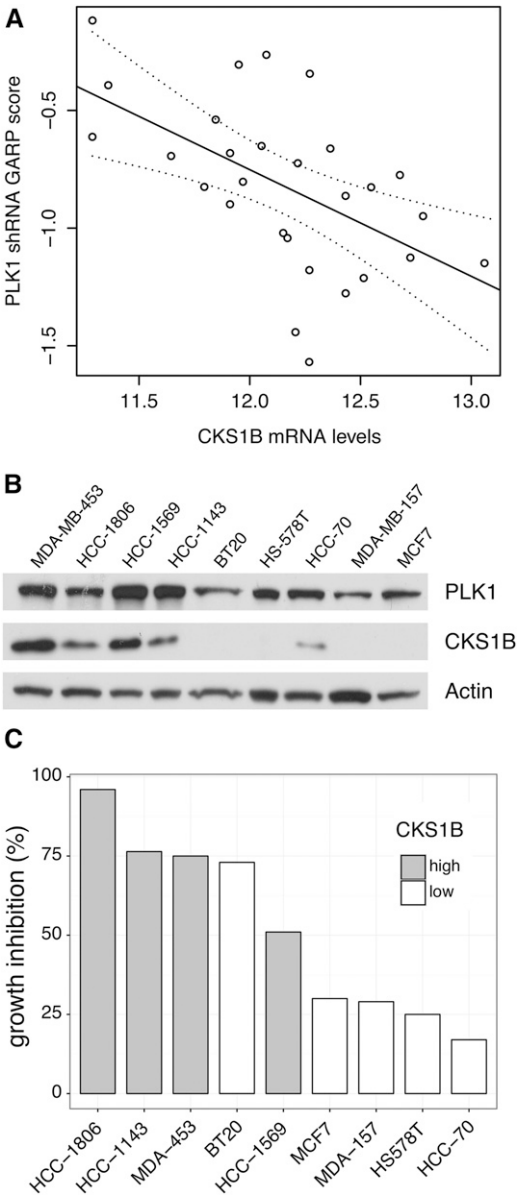

Figure 3 *CKS1B* expression in breast cancer cell lines affects sensitivity to *PLK1* knockdown. (A) The correlation of shRNA knockdown of PLK1 across 28 breast cancer cell lines with CKS1B expression. CKS1B expression data are from microarray expression analysis and were obtained from the Cancer Cell Line Encyclopedia. The GARP score is a measure reflecting growth inhibition caused by *PLK1* knockdown. (B) Protein extracts from the indicated breast cancer cell lines were assayed by protein blot for levels of CKS1B and PLK1 expression. An actin immunoblot serves as a loading control. The samples were grouped into cell lines with high CKS1B levels (left 4) and cell lines with low CKS1B levels (right 5). (C) The nine cancer cells lines in B were infected with shPLK1 lentivirus coexpressing RFP and selected with puromycin and then mixed with uninfected parent cells. The knockdown of *PLK1* was induced with doxycycline. Growth inhibition was calculated as the relative RFP^+ population at day 5 compared to day 2. High *vs.* low expression of CKS1B was determined from the protein blot (B) and is indicated by shaded or open bars, respectively.

(Barretina *et al.* 2012). Doxycycline induced efficient *PLK1* knockdown in most cell lines (Figure S5, A–C). In a competition assay, growth inhibition by *PLK1* knockdown was calculated as the relative RFP^+ population at day 5 compared to day 2 postinduction (Figure 3C). Cell lines were classified as high or low *CKS1B* expression based on the immunoblot results (shaded or open bars, respectively). The median inhibition of cell lines with high *CKS1B* expression is 76% compared to 29% for the cell lines with low *CKS1B* expression. This correlation between cellular levels of CKS1B and sensitivity to knockdown of *PLK1* is consistent with a synthetic interaction between *PLK1* and *CKS1B*.

We next examined whether increasing CKS1B levels in a cell line with low CKS1B would result in increased sensitivity to *PLK1* knockdown. We transfected an HS578T cell line that contained a doxycycline-inducible *PLK1*-shRNA with a lentivirus constitutively expressing *CKS1B* (Figure 4A). PLK1 protein levels were efficiently reduced by shRNA induction with or without *CKS1B* overexpression (compare DOX^- to DOX^+ in Figure 4A). Without *PLK1* knockdown, overexpression of *CKS1B* does not affect cell growth in a competition experiment: compare uninduced control cells (shaded) to *CKS1* overexpression (solid) in Figure 4B. Cell growth is inhibited by *PLK1* knockdown and *CKS1B* overexpression exacerbates this inhibition: compare control cells (shaded) to CKS1 overexpression (solid) in Figure 4B. Since *PLK1* knockdown also induces apoptosis (Liu and Erikson 2003), we monitored cell surface phosphatidylserine by Annexin V staining to visualize apoptotic cells under *PLK1* knockdown conditions with or without *CKS1B* overexpression. In line with its effect on growth, knockdown of *PLK1* in HS578T cells in the absence of overexpression increases the number of apoptotic cells in culture from a mean background value of 5% in the controls to a mean of 15% in the *PLK1* knockdown cells (uninduced, Figure S6). There is a small, but consistent increase in apoptosis after *PLK1* is knocked down in cells overexpressing *CKS1B* (Figure S6).

We further explored the effect on apoptosis after exposure to the selective PLK1 inhibitor Volasertib in HS578T cells where *CKS1B* is overexpressed (Rudolph *et al.* 2009). Similar to the knockdown experiment, in the absence of *CKS1B* overexpression, PLK1 inhibition increased the number of apoptotic cells in culture from an ~5% background to >40% at 20 nM Volasertib (Figure 4C). Importantly, cells that overexpress *CKS1B* show a significant increase in apoptosis after 20 nM Volasertib compared to the vector control (Figure 4C).

Finally, we manipulated a primary cell line, hMECs, to observe the interaction of *CKS1B* overexpression and *PLK1* knockdown in nontransformed cells (Figure S7). Like the HS578 cells, hMECs overexpressing *CKS1B* exhibit increased growth inhibition upon *PLK1* knockdown (Figure S7A). Figure S7B shows that the same hMECs overexpressing *CKS1B* show increased apoptosis upon *PLK1* knockdown. Surprisingly, knockdown of *CKS1B* provides a protective effect from *PLK1* knockdown (Figure S7, A and B). Thus, in a variety of cell lines, PLK1 inhibition by either gene expression knockdown or by a selective drug inhibitor shows a synthetic interaction with overexpressed *CKS1B* mimicking the interaction observed in yeast between *CKS1* and *cdc5*.

WEE1 and PLK1 inhibitors show a less than additive effect on apoptosis

Yeast mitotic entry is under the control of the Swe1 tyrosine kinase that inhibits the CDK, Cdc28. Swe1 is degraded in a pathway that depends on the polo-like kinase Cdc5 (see Figure 1A). We show above that deletion of the *SWE1* gene suppresses the effect of *CKS1* overexpression in a cdc5 mutant cell. This observation leads to a prediction that the effect of inhibition of PLK1 and WEE1 will not be independent, *i.e.*, epistatic. In human cells, an epistatic relationship is characterized as antagonistic, *i.e.*, a less than additive effect. We therefore treated breast cancer cell lines with the PLK1 inhibitor Volasertib and the WEE1 inhibitor MK-1775 (Hirai *et al.* 2009), alone or in combination (Figure 5 and Figure S8). We then calculated the additive effect of dual drug treatment using the Bliss model (see *Materials and Methods*) and compared this result to the observed effect on cells treated with both drugs (Bliss 1939). In every replicate experiment in both the HCC1569 and HCC1806 cell lines, the percent apoptosis induced by the combined treatment is smaller than the predicted additive effect (Figure 5). A paired samples *t*-test was performed for the merged data for the two strains giving a *P*-value = 0.015. The less than additive effect of the combined drug treatment suggests that their targets, WEE1 and PLK1, like their yeast counterparts, function in the same cellular pathways, demonstrating a conserved relationship from yeast to humans.

Discussion

In cancer cells, gene amplifications often occur that affect cell growth and function; however, it is difficult to predict which pathways can be targeted therapeutically. By defining SDL interactions for an overexpressed gene, the functions and/or pathways that are important to modulate cell viability or growth are identified. Thus, targeting any of the down-regulated genes in the SDL interaction can provide a mechanism to inhibit the growth of cancer cells that overexpress a gene. In that context, the driver status of the amplified gene does not matter. To rapidly identify such SDL interactions, we take advantage of the ease, speed, and cost efficiency of yeast genetics to systematically search for SDL interactions.

CKS1B, a conserved component of CDK, is amplified in multiple cancers and its involvement in multiple cell cycle processes suggests a role in oncogenesis. However, the consequences of increased *CKS1B* expression are unclear, due to both positive and negative effects of CKS1 on cell cycle progression (Dunphy and Newport 1989; Patra and Dunphy 1996; Patra *et al.* 1999). Our systematic genetic approach in yeast defines the consequence of *CKS1* expression by identifying mutations that fail to tolerate increased expression of *CKS1*. The genetic screen identified a number of mutations

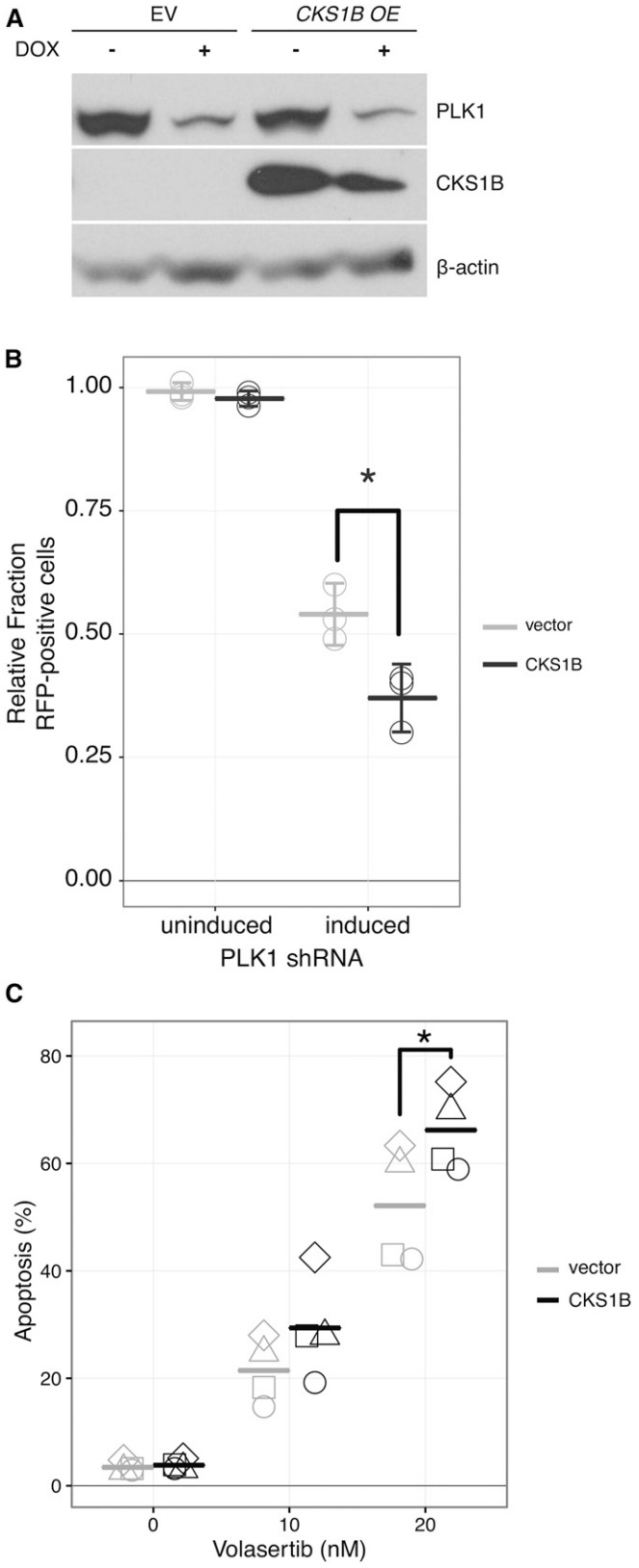

Figure 4 *CKS1B* overexpression increases the cellular sensitivity to PLK1 inhibition. (A) Protein blot showing levels of PLK1 and CKS1B in HS578T cells. Induction of PLK1-shRNA by doxycycline (DOX) is indicated by − for uninduced or + for induced. CKS1B expression is low in the control cells (EV, empty vector) and abundant in cells with a *CKS1B* overexpression clone. (B) GFP+ CKS1B overexpression or control HS578T-shPLK1 cells were mixed 1:1 with parent cells, and then PLK1 shRNA was induced with doxycycline. Growth inhibition was calculated as the relative RFP/GFP+ population at day 5 compared to day 2. The *t*-test comparing growth with and without *CKS1B* overexpression results in * *P*-value = 0.023. (C) HS578T cells were treated with the PLK1 inhibitor Volasertib (BI 6727) and assayed for Annexin V APC staining to measure the fraction of apoptotic cells. Percent apoptosis between vector and *CKS1B*-overexpressing cells was calculated and plotted for each drug concentration to show the effect of CKS1B expression on apoptosis during PLK1 inhibition. Pairwise analysis of apoptosis indicates a significant increase in apoptosis in the context of CKS1B overexpression (*P*-value = 0.005).

that affect cell cycle progression in G2 and M cell cycle phases, but particularly identified genes affecting the transitions between G2–M (mitotic entry) and M–G1 (mitotic exit). Subsequent genetic analyses show that these SDL interactions depend on the activity of two important CDK inhibitors, Swe1 and Sic1.

CKS1 has long been recognized as an essential component of cyclin–CDK complexes, but its role in these complexes is only recently coming into focus. A structural model of CKS1 in a cyclin–CDK complex predicts that a highly conserved anion binding pocket on CKS1 orients to the same face of the complex as the CDK active site, suggesting that CKS1 provides additional substrate binding specificity (Arvai *et al.* 1995; Bourne *et al.* 1996). Moreover, it has recently been shown that CKS1 binds phosphothreonine-containing consensus sites that allow the CDK complex to processively phosphorylate suboptimal CDK consensus sites (Kõivomägi *et al.* 2011; Koivomagi *et al.* 2013; McGrath *et al.* 2013). Interestingly, Swe1 and Sic1 are phosphorylated by CDK and each contains CKS1 phosphothreonine consensus sites.

During a normal cell cycle, the kinase activity of Swe1 is activated by multiple CDK-dependent phosphorylations, stimulating its inhibitory phosphorylation of CDK at tyrosine 19 - (Harvey *et al.* 2005, 2011) (Figure 1B). Phosphorylated Swe1 interacts directly with Hsl7, which is localized to the septin ring in a complex with Hsl1 and Elm1 proteins (Theesfeld *et al.* 2003; Howell and Lew 2012). At the septin ring, Swe1 is additionally phosphorylated by Cdc5 to promote its degradation (Sakchaisri *et al.* 2004; Howell and Lew 2012). The *elm1*, *hsl1*, and *hsl7* mutations all result in mislocalization and stabilization of Swe1, leading to a G2–M delay and a mild slow growth phenotype, but not a complete cell cycle arrest (Barral *et al.* 1999; Longtine *et al.* 2000). It is thought that the mild arrest phenotype is due to the action of multiple phosphatases that reverse the activating phosphorylations on SWE1 and/or the inhibitory phosphorylation on CDK (Harvey *et al.* 2011; Howell and Lew 2012). Indeed, *elm1* and *hsl7* mutations are lethal when combined with loss of the Mih1 phosphatase (McMillan *et al.* 1999). Deletion of Swe1 or mutating the site that it phosphorylates on Cdc28, tyrosine 19, both suppress this lethality (McMillan *et al.* 1999). These results show that CDK dephosphorylation is

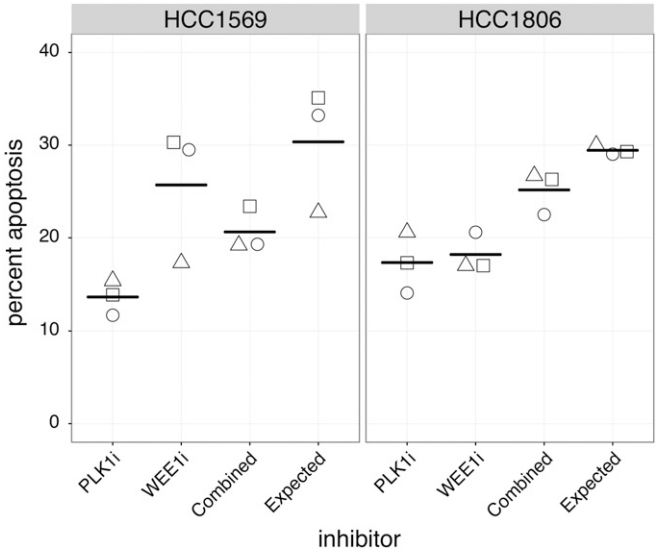

Figure 5 Combined inhibition of PLK1 and WEE1 in breast cancer cell lines is less than additive. HCC1569 and HCC1806 cell lines were treated with 100 nM of the PLK1 inhibitor Volasertib, 400 nM of the WEE1 inhibitor MK-1775, or the WEE1 and PLK1 inhibitors together (combined), and the fraction of apoptotic cells was determined as in Figure 4. Background apoptosis in the untreated cell lines was subtracted out, and an additive effect of dual drug treatment was calculated based on the Bliss independence model (expected). Replicate experiments in individual cell lines are distinguished by plot symbols.

essential in those double mutants (Szkotnicki *et al.* 2008). These observations support a negative feedback model of CDK activity via Swe1 that is limited by Swe1 degradation during a normal cell cycle. Thus, when cells fail to form a septin ring, mitotic entry is blocked due to stabilization of Swe1 and its inhibitory phosphorylation of CDK (Howell and Lew 2012). This checkpoint mechanism also accounts for the Swe1 dependence of *elm1*, *hsl1*, and *hsl7* SDL interactions with overexpressed *CKS1* (Figure 1C). We argue that excess Cks1 protein shifts the equilibrium so that more Swe1 binds to the CDK complex, causing sustained negative regulation of the CDK and resulting in complete arrest when Swe1 cannot be degraded. As described above for the *elm1-mih1 and hsl7-mih1* synthetic lethality, the Cdc28 tyrosine 19 mutation suppresses the *CKS1* SDLs with *hsl1*, *hsl7*, and *elm1* (Figure 1C). Thus, the mechanism behind this SDL is not due to some other target of Swe1 phosphorylation, but rather directly to the Swe1 inhibitory phosphorylation of CDK.

We noted that *swe1* deletion only partially suppressed the sensitivity of the polo-like kinase *cdc5* mutant (Figure S2D and Figure 1D). Additionally, *SWE1* deletion did not suppress the *CKS1* SDL with any of the mutations in the mitotic exit network (Figure S4A). The yeast mitotic exit network ensures that cells enter G1 only after spindle elongation in anaphase (reviewed in Bardin and Amon 2001). Spindle elongation activates the GTPase Tem1, which triggers a signal cascade leading to activation of the phosphatase Cdc14. Cdc14 dephosphorylates Cdh1, a specificity factor for the APC, leading to degradation of the mitotic cyclins (Bardin and Amon 2001). Cdc14-dependent dephosphorylation also activates the transcription factor Swi5, leading to expression of the CDK inhibitor Sic1, which also contains Cks1 consensus binding sites that affect its CDK-dependent phosphorylation (Kõivomägi *et al.* 2011; McGrath *et al.* 2013). Furthermore, Cdc14 dephosphorylates Sic1 itself, leading to its stabilization (Jaspersen *et al.* 1998; Visintin *et al.* 1998). Therefore Sic1, although not an essential CDK inhibitor, plays a parallel role to the APC by inhibiting any residual CDK activity. In fact, *SIC1* becomes essential when components of the mitotic exit network are mutated (Chatr-Aryamontri *et al.* 2015), whereas overexpression of *SIC1* ameliorates the effect of mutations in the mitotic exit network pathway (Jaspersen *et al.* 1998). Similar to our model of the Cks1 effect on Swe1, we propose that increased levels of Cks1 stabilize the association of the CDK with Sic1. However, in this case, the association drives phosphorylation and degradation of Sic1 limiting its ability to inhibit the CDK, inactivation of which is essential for mitotic exit. This model is supported by the observation that the SDL interactions between overexpressed *CKS1* and mutations in the mitotic exit network pathway are suppressed by overexpression of Sic1 (Figure 2B and Figure S3C).

The effects of Cks1 overexpression on the Swe1 and Sic CDK inhibitors explain many of the genetic interactions identified in this study. However, it is likely that excess Cks1 affects CDK targeting to multiple substrates involved in cell cycle progression. Additional studies will be necessary to identify more of these factors. Nevertheless, we did identify an important candidate gene, the polo-like kinase Cdc5, which is involved in both mitotic entry and mitotic exit (Figure 1B and Figure 2A). This gene is conserved in mammalian cells and has been targeted for therapeutic development (Degenhardt and Lampkin 2010). Mutual exclusion analysis revealed that the human homolog of Cdc5, PLK1, is rarely down-regulated when *CKS1B* is overexpressed. Furthermore, multiple experiments show that human cells with increased *CKS1B* expression exhibit decreased growth and increased apoptosis upon PLK1 inhibition by either shRNA or with the specific PLK1 inhibitor Volasertib (Figure 3, Figure 4, Figure S5, Figure S6, and Figure S7). Thus, despite the evolutionary distance between yeast and humans, the SDL interaction we identified in yeast is conserved in humans. In addition, our yeast studies show that Swe1 functions in the mitotic entry pathway with Cdc5. We also showed that this epistatic relationship is conserved, since the combined inhibition of the mammalian counterparts of the Swe1 and Cdc5 kinases, WEE1 and PLK1, respectively, exhibit a less than additive effect on apoptosis (Figure 5). Since WEE1 and PLK1 inhibitors are both in clinical development to treat cancers, our data argue that combining these agents would not be clinically efficacious. Furthermore, although additional preclinical and clinical testing is required, our data support the hypothesis that CKS1 overexpression is one predictive biomarker of sensitivity to PLK1 inhibitors.

Acknowledgments

We thank Brenda Andrews (University of Toronto) for sharing the library of temperature-sensitive alleles in the BY4741 background. We thank Michael Smith for critical reading of the manuscript. R.R. and M.M. received support from the New York State Department of Health, Wadsworth Center Health Research Science Board (http://www.wadsworth.org/extramural, HRSB-C028248). R.R. received support from the National Cancer Institute (NCI) (R33 CA125520) and the National Institute of General Medical Sciences (R37 GM050237). M.M. received support from the Southwest Oncology Group (SWOG) (SWOG CU12-0734 SC1) and the American Association of Cancer Research (SU2C-AACR-DT0209). E.B. and J.D. received support from a NCI training grant (T32 CA009503). The funders had no role in study design, data collection and analysis, decision to publish, or preparation of the manuscript.

Literature Cited

Alvaro, D., M. Lisby, and R. Rothstein, 2007 Genome-wide analysis of Rad52 foci reveals diverse mechanisms impacting recombination. PLoS Genet. 3: e228.

Arvai, A. S., Y. Bourne, M. J. Hickey, and J. A. Tainer, 1995 Crystal structure of the human cell cycle protein CksHs1: single domain fold with similarity to kinase N-lobe domain. J. Mol. Biol. 249: 835–842.

Barberis, M., L. De Gioia, M. Ruzzene, S. Sarno, P. Coccetti *et al.*, 2005 The yeast cyclin-dependent kinase inhibitor Sic1 and mammalian p27(Kip1) are functional homologues with a structurally conserved inhibitory domain. Biochem. J. 387: 639–647.

Bardin, A. J., and A. Amon, 2001 Men and sin: What's the difference? Nat. Rev. Mol. Cell Biol. 2: 815–826.

Barral, Y., M. Parra, S. Bidlingmaier, and M. Snyder, 1999 Nim1-related kinases coordinate cell cycle progression with the organization of the peripheral cytoskeleton in yeast. Genes Dev. 13: 176–187.

Barretina, J., G. Caponigro, N. Stransky, K. Venkatesan, A. A. Margolin *et al.*, 2012 The Cancer Cell Line Encyclopedia enables predictive modelling of anticancer drug sensitivity. Nature 483: 603–607.

Bliss, C. I., 1939 The toxicity of poisons applied jointly. Ann. Appl. Biol. 26: 585–615.

Booher, R. N., R. J. Deshaies, and M. W. Kirschner, 1993 Properties of *Saccharomyces cerevisiae wee1* and its differential regulation of p34/CDC28 in response to G1 and G2 cyclins. EMBO J. 12: 3417–3426.

Bourne, Y., M. H. Watson, M. J. Hickey, W. Holmes, W. Rocque *et al.*, 1996 Crystal structure and mutational analysis of the human CDK2 kinase complex with cell cycle-regulatory protein CksHs1. Cell 84: 863–874.

Bourne, Y., M. H. Watson, A. S. Arvai, S. L. Bernstein, S. I. Reed *et al.*, 2000 Crystal structure and mutational analysis of the *Saccharomyces cerevisiae* cell cycle regulatory protein Cks1: implications for domain swapping, anion binding and protein interactions. Structure 8: 841–850.

Brizuela, L., G. Draetta, and D. Beach, 1987 p13/suc1 acts in the fission yeast cell division cycle as a component of the p34/cdc2 protein kinase. EMBO J. 6: 3507–3514.

Butt, T. R., E. J. Sternberg, J. A. Gorman, P. Clark, D. Hamer *et al.*, 1984 Copper metallothionein of yeast, structure of the gene, and regulation of expression. Proc. Natl. Acad. Sci. USA 81: 3332–3336.

Cerami, E., J. Gao, U. Dogrusoz, B. E. Gross, S. O. Sumer *et al.*, 2012 The cBio cancer genomics portal: an open platform for exploring multidimensional cancer genomics data. Cancer Discov. 2: 401–404.

Chang, J., N.-G. Kim, Z. Piao, C. Park, K.-S. Park *et al.*, 2002 Assessment of chromosomal losses and gains in hepatocellular carcinoma. Cancer Lett. 182: 193–202.

Chatr-Aryamontri, A., B. J. Breitkreutz, R. Oughtred, L. Boucher, S. Heinicke *et al.*, 2015 The BioGRID interaction database: 2015 update. Nucleic Acids Res. 43: D470–D478.

Chen, L., T. H. Chan, and X. Y. Guan, 2010 Chromosome 1q21 amplification and oncogenes in hepatocellular carcinoma. Acta Pharmacol. Sin. 31: 1165–1171.

Christianson, T. W., R. S. Sikorski, M. Dante, J. H. Shero, and P. Hieter, 1992 Multifunctional yeast high-copy-number shuttle vectors. Gene 110: 119–122.

Cid, V. J., M. J. Shulewitz, K. L. McDonald, and J. Thorner, 2001 Dynamic localization of the Swe1 regulator Hsl7 during the *Saccharomyces cerevisiae* cell cycle. Mol. Biol. Cell 12: 1645–1669.

Degenhardt, Y., and T. Lampkin, 2010 Targeting Polo-like kinase in cancer therapy. Clin. Cancer Res. 16: 384–389.

Dittmar, J. C., R. J. D. Reid, and R. Rothstein, 2010 ScreenMill: a freely available software suite for growth measurement, analysis and visualization of high-throughput screen data. BMC Bioinformatics 11: 353.

Dittmar, J. C., S. Pierce, R. Rothstein, and R. J. D. Reid, 2013 Physical and genetic-interaction density reveals functional organization and informs significance cutoffs in genome-wide screens. Proc. Natl. Acad. Sci. USA 110: 7389–7394.

Draetta, G., L. Brizuela, J. Potashkin, and D. Beach, 1987 Identification of p34 and p13, human homologs of the cell cycle regulators of fission yeast encoded by *cdc2+* and *suc1+*. Cell 50: 319–325.

Dunphy, W. G., and J. W. Newport, 1989 Fission yeast p13 blocks mitotic activation and tyrosine dephosphorylation of the *Xenopus* cdc2 protein kinase. Cell 58: 181–191.

Ganoth, D., G. Bornstein, T. K. Ko, B. Larsen, M. Tyers *et al.*, 2001 The cell-cycle regulatory protein Cks1 is required for SCFSkp2-mediated ubiquitinylation of p27. Nat. Cell Biol. 3: 321–324.

Gorman, J. A., P. E. Clark, M. C. Lee, C. Debouck, and M. Rosenberg, 1986 Regulation of the yeast metallothionein gene. Gene 48: 13–22.

Hadwiger, J. A., C. Wittenberg, M. D. Mendenhall, and S. I. Reed, 1989 The *Saccharomyces cerevisiae CKS1* gene, a homolog of the *Schizosaccharomyces pombe suc1+* gene, encodes a subunit of the Cdc28 protein kinase complex. Mol. Cell. Biol. 9: 2034–2041.

Harvey, S. L., and D. R. Kellogg, 2003 Conservation of mechanisms controlling entry into mitosis: budding yeast wee1 delays entry into mitosis and is required for cell size control. Curr. Biol. 13: 264–275.

Harvey, S. L., A. Charlet, W. Haas, S. P. Gygi, and D. R. Kellogg, 2005 Cdk1-dependent regulation of the mitotic inhibitor Wee1. Cell 122: 407–420.

Harvey, S. L., G. Enciso, N. Dephoure, S. P. Gygi, J. Gunawardena *et al.*, 2011 A phosphatase threshold sets the level of Cdk1 activity in early mitosis in budding yeast. Mol. Biol. Cell 22: 3595–3608.

Hayles, J., S. Aves, and P. Nurse, 1986a *suc1* is an essential gene involved in both the cell cycle and growth in fission yeast. EMBO J. 5: 3373–3379.

Hayles, J., D. Beach, B. Durkacz, and P. Nurse, 1986b The fission yeast cell cycle control gene *cdc2*: isolation of a sequence *suc1*

that suppresses *cdc2* mutant function. Mol. Gen. Genet. 202: 291–293.

Herrero, E., and P. H. Thorpe, 2016 Synergistic control of kinetochore protein levels by Psh1 and Ubr2. PLoS Genet. 12: e1005855.

Hirai, H., Y. Iwasawa, M. Okada, T. Arai, T. Nishibata *et al.*, 2009 Small-molecule inhibition of Wee1 kinase by MK-1775 selectively sensitizes p53-deficient tumor cells to DNA-damaging agents. Mol. Cancer Ther. 8: 2992–3000.

Howell, A. S., and D. J. Lew, 2012 Morphogenesis and the cell cycle. Genetics 190: 51–77.

Huang, C.-W., C.-Y. Lin, H.-Y. Huang, H.-W. Liu, Y.-J. Chen *et al.*, 2010 CKS1B overexpression implicates clinical aggressiveness of hepatocellular carcinomas but not p27(Kip1) protein turnover: An independent prognosticator with potential p27 (Kip1)-independent oncogenic attributes? Ann. Surg. Oncol. 17: 907–922.

Jaspersen, S. L., J. F. Charles, R. L. Tinker-Kulberg, and D. O. Morgan, 1998 A late mitotic regulatory network controlling cyclin destruction in *Saccharomyces cerevisiae*. Mol. Biol. Cell 9: 2803–2817.

Koivomagi, M., M. Ord, A. Iofik, E. Valk, R. Venta *et al.*, 2013 Multisite phosphorylation networks as signal processors for Cdk1. Nat. Struct. Mol. Biol. 20: 1415–1424.

Kõivomägi, M., E. Valk, R. Venta, A. Iofik, M. Lepiku *et al.*, 2011 Cascades of multisite phosphorylation control Sic1 destruction at the onset of S phase. Nature 480: 128–131.

León Ortiz, A. M., R. J. D. Reid, J. C. Dittmar, R. Rothstein, and A. Nicolas, 2011 Srs2 overexpression reveals a helicase-independent role at replication forks that requires diverse cell functions. DNA Repair (Amst.) 10: 506–517.

Li, Z., F. J. Vizeacoumar, S. Bahr, J. Li, J. Warringer *et al.*, 2011 Systematic exploration of essential yeast gene function with temperature-sensitive mutants. Nat. Biotechnol. 29: 361–367.

Liu, X., and R. L. Erikson, 2003 Polo-like kinase (Plk)1 depletion induces apoptosis in cancer cells. Proc. Natl. Acad. Sci. USA 100: 5789–5794.

Longtine, M. S., C. L. Theesfeld, J. N. McMillan, E. Weaver, J. R. Pringle *et al.*, 2000 Septin-dependent assembly of a cell cycle-regulatory module in *Saccharomyces cerevisiae*. Mol. Cell. Biol. 20: 4049–4061.

Marcotte, R., K. Brown, F. Suarez, and A. Sayad, K. Karamboulas *et al.*, 2012 Essential gene profiles in breast, pancreatic, and ovarian cancer cells. Cancer Discov. 2: 172–189.

McGrath, D. A., E. R. M. Balog, M. Kõivomägi, R. Lucena, M. V. Mai *et al.*, 2013 Cks confers specificity to phosphorylation-dependent CDK signaling pathways. Nat. Struct. Mol. Biol. 20: 1407–1414.

McMillan, J. N., M. S. Longtine, R. A. Sia, C. L. Theesfeld, E. S. Bardes *et al.*, 1999 The morphogenesis checkpoint in *Saccharomyces cerevisiae*: cell cycle control of Swe1p degradation by Hsl1p and Hsl7p. Mol. Cell. Biol. 19: 6929–6939.

Measday, V., and P. Hieter, 2002 Synthetic dosage lethality. Methods Enzymol. 350: 316–326.

Morris, M. C., P. Kaiser, S. Rudyak, C. Baskerville, M. H. Watson *et al.*, 2003 Cks1-dependent proteasome recruitment and activation of CDC20 transcription in budding yeast. Nature 423: 1009–1013.

Patra, D., and W. G. Dunphy, 1996 Xe-p9, a *Xenopus* Suc1/Cks homolog, has multiple essential roles in cell cycle control. Genes Dev. 10: 1503–1515.

Patra, D., S. X. Wang, A. Kumagai, and W. G. Dunphy, 1999 The *Xenopus* Suc1/Cks protein promotes the phosphorylation of G2/M regulators. J. Biol. Chem. 274: 36839–36842.

Piatti, S., M. Venturetti, E. Chiroli, and R. Fraschini, 2006 The spindle position checkpoint in budding yeast: the motherly care of MEN. Cell Div. 1: 2.

Reid, R. J. D., S. González-Barrera, I. Sunjevaric, D. Alvaro, S. Ciccone *et al.*, 2011 Selective ploidy ablation, a high-throughput plasmid transfer protocol, identifies new genes affecting topoisomerase I-induced DNA damage. Genome Res. 21: 477–486.

Reynard, G. J., W. Reynolds, R. Verma, and R. J. Deshaies, 2000 Cks1 is required for G(1) cyclin-cyclin-dependent kinase activity in budding yeast. Mol. Cell. Biol. 20: 5858–5864.

Richardson, H. E., C. S. Stueland, J. Thomas, P. Russell, and S. I. Reed, 1990 Human cDNAs encoding homologs of the small p34Cdc28/Cdc2-associated protein of *Saccharomyces cerevisiae* and *Schizosaccharomyces pombe*. Genes Dev. 4: 1332–1344.

Rudolph, D., M. Steegmaier, M. Hoffmann, M. Grauert, A. Baum *et al.*, 2009 BI 6727, a Polo-like kinase inhibitor with improved pharmacokinetic profile and broad antitumor activity. Clin. Cancer Res. 15: 3094–3102.

Sakchaisri, K., S. Asano, L.-R. Yu, M. J. Shulewitz, C. J. Park *et al.*, 2004 Coupling morphogenesis to mitotic entry. Proc. Natl. Acad. Sci. USA 101: 4124–4129.

Santarius, T., J. Shipley, D. Brewer, M. R. Stratton, and C. S. Cooper, 2010 A census of amplified and overexpressed human cancer genes. Nat. Rev. Cancer 10: 59–64.

Schiestl, R. H., and R. D. Gietz, 1989 High efficiency transformation of intact yeast cells using single stranded nucleic acids as a carrier. Curr. Genet. 16: 339–346.

Sherman, F., G. R. Fink and J. B. Hicks, 1986 *Laboratory Course Manual for Methods in Yeast Genetics*. Cold Spring Harbor Laboratory Press, Cold Spring Harbor, NY.

Sia, R. A., E. S. Bardes, and D. J. Lew, 1998 Control of Swe1p degradation by the morphogenesis checkpoint. EMBO J. 17: 6678–6688.

Slotky, M., M. a. Shapira, O. Ben-Izhak, S. Linn, B. Futerman *et al.*, 2005 The expression of the ubiquitin ligase subunit Cks1 in human breast cancer. BCR 7: R737–R744.

Spruck, C., H. Strohmaier, M. Watson, A. P. Smith, A. Ryan *et al.*, 2001 A CDK-independent function of mammalian Cks1: targeting of SCFSkp2 to the CDK inhibitor p27Kip1. Mol. Cell 7: 639–650.

Szkotnicki, L., J. M. Crutchley, T. R. Zyla, E. S. Bardes, and D. J. Lew, 2008 The checkpoint kinase Hsl1p is activated by Elm1p-dependent phosphorylation. Mol. Biol. Cell 19: 4675–4686.

Tang, Y., and S. I. Reed, 1993 The Cdk-associated protein Cks1 functions both in G1 and G2 in Saccharomyces cerevisiae. Genes Dev. 7: 822–832.

The Cancer Genome Atlas Network, 2012 Comprehensive molecular portraits of human breast tumours. Nature 490: 61–70.

Theesfeld, C. L., T. R. Zyla, E. G. Bardes, and D. J. Lew, 2003 A monitor for bud emergence in the yeast morphogenesis checkpoint. Mol. Biol. Cell 14: 3280–3291.

Thomas, B. J., and R. Rothstein, 1989 The genetic control of direct-repeat recombination in *Saccharomyces*: the effect of *rad52* and *rad1* on mitotic recombination at *GAL10*, a transcriptionally regulated gene. Genetics 123: 725–738.

Toyn, J. H., A. L. Johnson, J. D. Donovan, W. M. Toone, and L. H. Johnston, 1997 The Swi5 transcription factor of *Saccharomyces cerevisiae* has a role in exit from mitosis through induction of the cdk-inhibitor Sic1 in telophase. Genetics 145: 85–96.

Unni, A. M., W. W. Lockwood, K. Zejnullahu, S. Q. Lee-Lin, and H. Varmus, 2015 Evidence that synthetic lethality underlies the mutual exclusivity of oncogenic KRAS and EGFR mutations in lung adenocarcinoma. eLife 4: e06907.

Visintin, R., K. Craig, E. S. Hwang, S. Prinz, M. Tyers *et al.*, 1998 The phosphatase Cdc14 triggers mitotic exit by reversal of Cdk-dependent phosphorylation. Mol. Cell 2: 709–718.

Visintin, R., F. Stegmeier, and A. Amon, 2003 The role of the polo kinase Cdc5 in controlling Cdc14 localization. Mol. Biol. Cell 14: 4486–4498.

Vogelstein, B., N. Papadopoulos, V. E. Velculescu, S. Zhou, L. A. Diaz, Jr. *et al.*, 2013 Cancer genome landscapes. Science 339: 1546–1558.

Wagner, M., G. Price, and R. Rothstein, 2006 The absence of Top3 reveals an interaction between the Sgs1 and Pif1 DNA helicases in *Saccharomyces cerevisiae*. Genetics 174: 555–573.

Winzeler, E. A., D. D. Shoemaker, A. Astromoff, H. Liang, K. Anderson *et al.*, 1999 Functional characterization of the *S. cerevisiae* genome by gene deletion and parallel analysis. Science 285: 901–906.

Zitouni, S., C. Nabais, S. C. Jana, A. Guerrero, and M. Bettencourt-Dias, 2014 Polo-like kinases: structural variations lead to multiple functions. Nat. Rev. Mol. Cell Biol. 15: 433–452.

Communicating editor: A. Murray

Figure S1

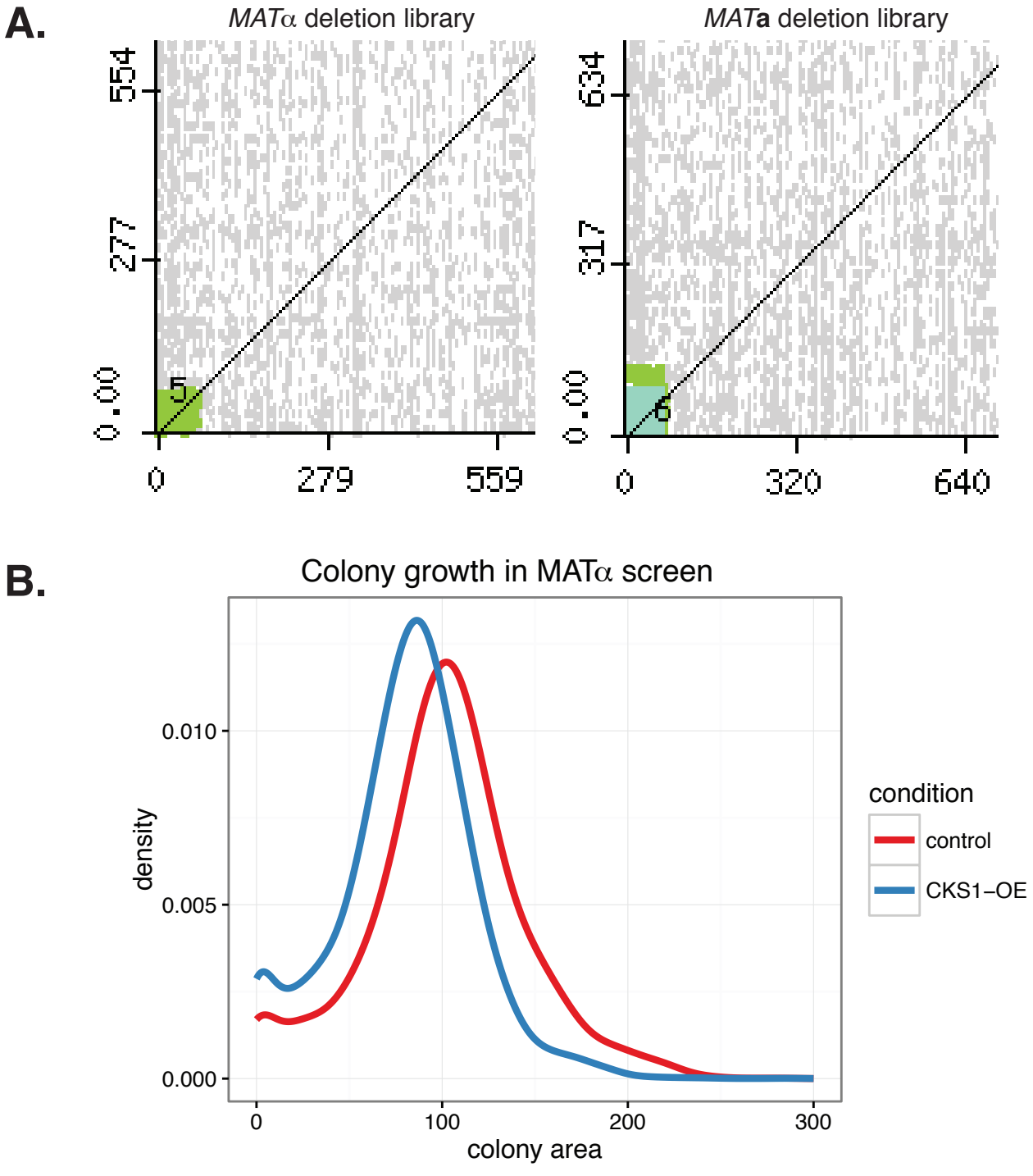
A.
MATα deletion library
MATa deletion library
554
277
0.00
5
0
279
559
634
317
0.00
6
0
320
640
B.
Colony growth in MATα screen
0.010
0.005
0.000
density
0
100
200
300
colony area
condition
control
CKS1−OE

Figure S2

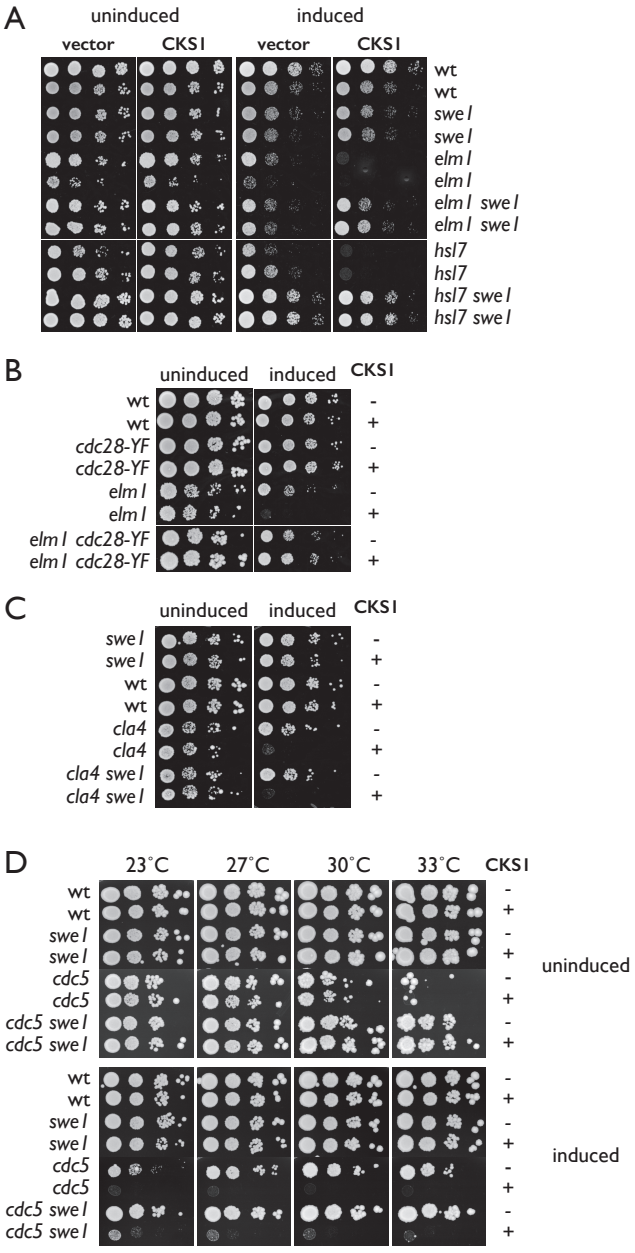
A
uninduced
induced
vector
CKS1
vector
CKS1
wt
wt
swe1
swe1
elm1
elm1
elm1 swe1
elm1 swe1
hsl7
hsl7
hsl7 swe1
hsl7 swe1
B
uninduced
induced
CKS1
wt -
wt +
cdc28-YF -
cdc28-YF +
elm1 -
elm1 +
elm1 cdc28-YF -
elm1 cdc28-YF +
C
uninduced
induced
CKS1
swe1 -
swe1 +
wt -
wt +
cla4 -
cla4 +
cla4 swe1 -
cla4 swe1 +
D
23˚C
27˚C
30˚C
33˚C
CKS1
wt -
wt +
swe1 -
swe1 +
cdc5 -
cdc5 +
cdc5 swe1 -
cdc5 swe1 +
uninduced
wt -
wt +
swe1 -
swe1 +
cdc5 -
cdc5 +
cdc5 swe1 -
cdc5 swe1 +
induced

Figure S3

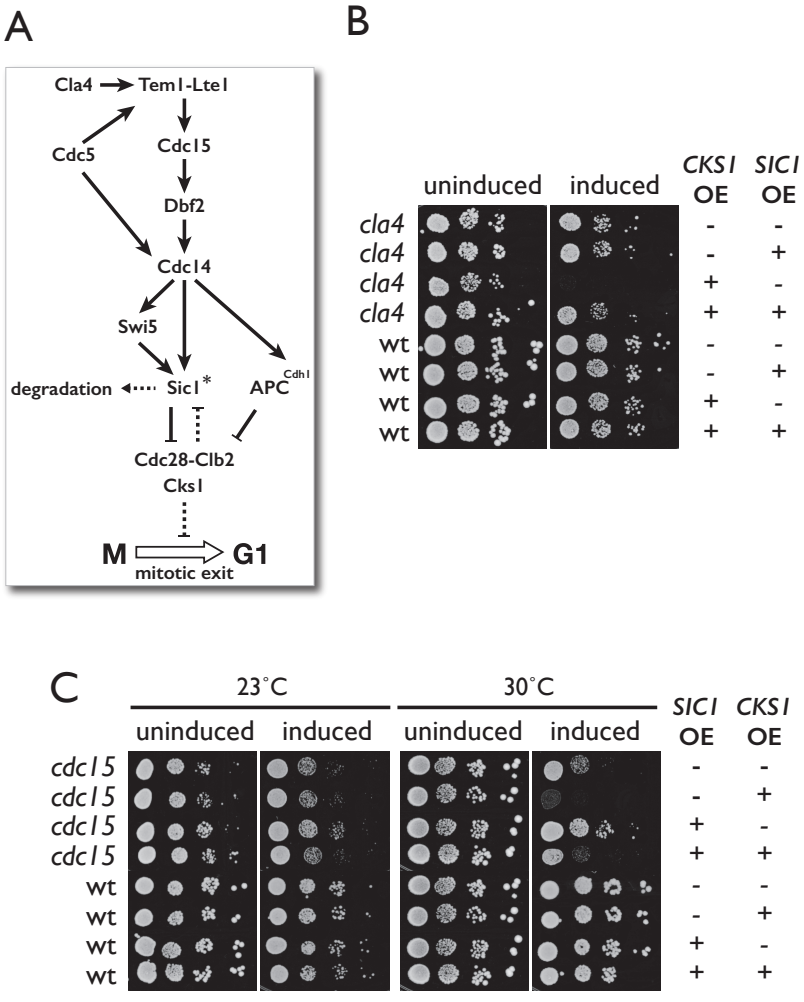
A
Cla4
Tem1-Lte1
Cdc5
Cdc15
Dbf2
Cdc14
Swi5
degradation
Sic1*
APC Cdh1
Cdc28-Clb2
Cks1
M
G1
mitotic exit
B
uninduced
induced
CKS1 OE
SIC1 OE
cla4 - -
cla4 - +
cla4 + -
cla4 + +
wt - -
wt - +
wt + -
wt + +
C
23˚C
30˚C
uninduced
induced
uninduced
induced
SIC1 OE
CKS1 OE
cdc15 - -
cdc15 - +
cdc15 + -
cdc15 + +
wt - -
wt - +
wt + -
wt + +

Figure S4

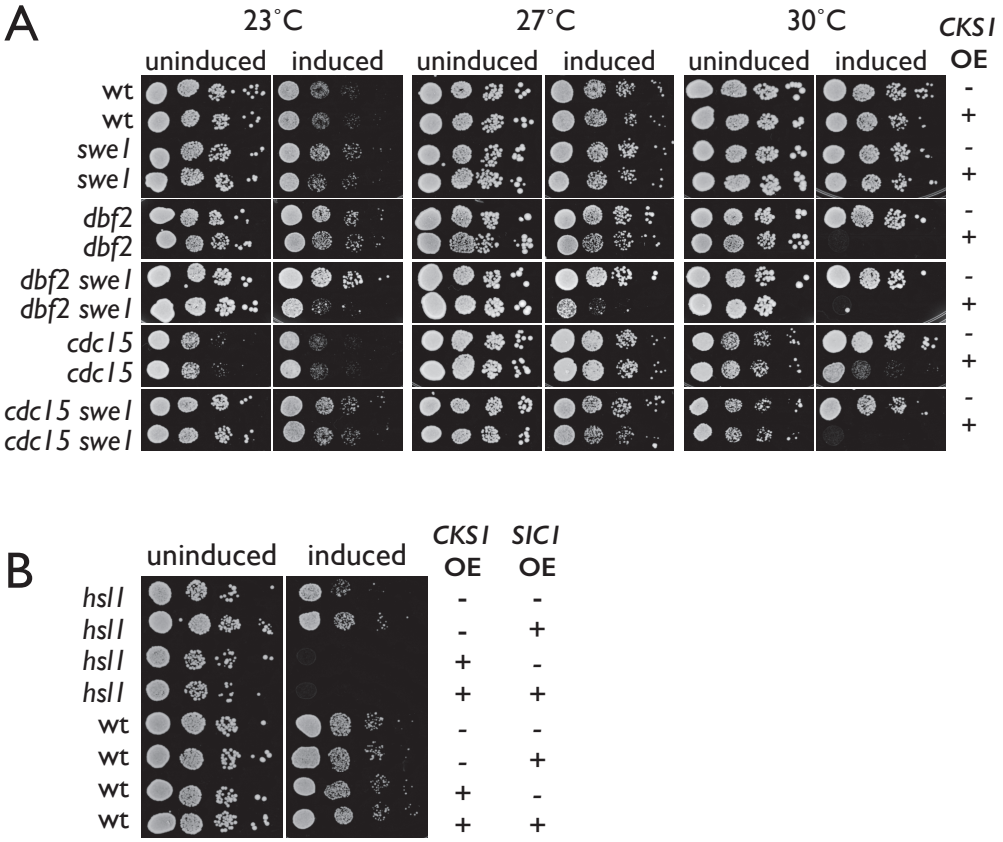
A
23˚C
27˚C
30˚C
uninduced
induced
uninduced
induced
uninduced
induced
CKS1 OE
wt
wt
swe1
swe1
dbf2
dbf2
dbf2 swe1
dbf2 swe1
cdc15
cdc15
cdc15 swe1
cdc15 swe1
B
uninduced
induced
CKS1 OE
SIC1 OE
hsl1
wt

Figure S5

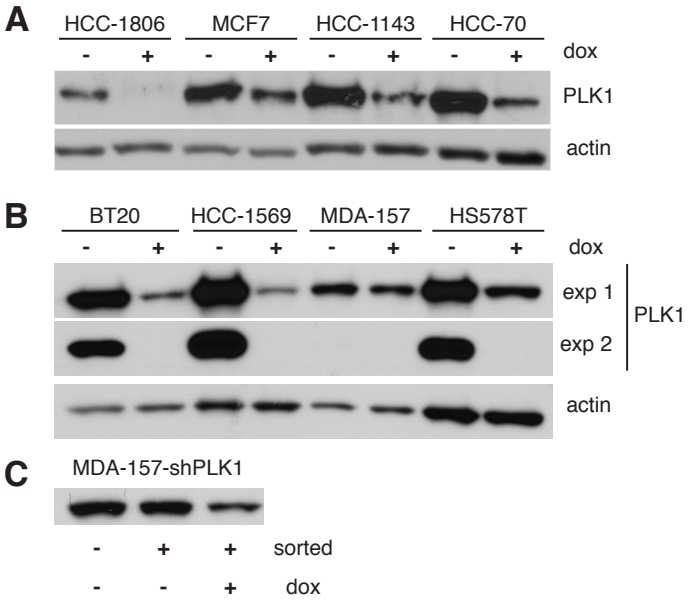
A
HCC-1806
MCF7
HCC-1143
HCC-70
- + - + - + - +
dox
PLK1
actin
B
BT20
HCC-1569
MDA-157
HS578T
- + - + - + - +
dox
exp 1
exp 2
PLK1
actin
C
MDA-157-shPLK1
- + + sorted
- - + dox

Figure S6

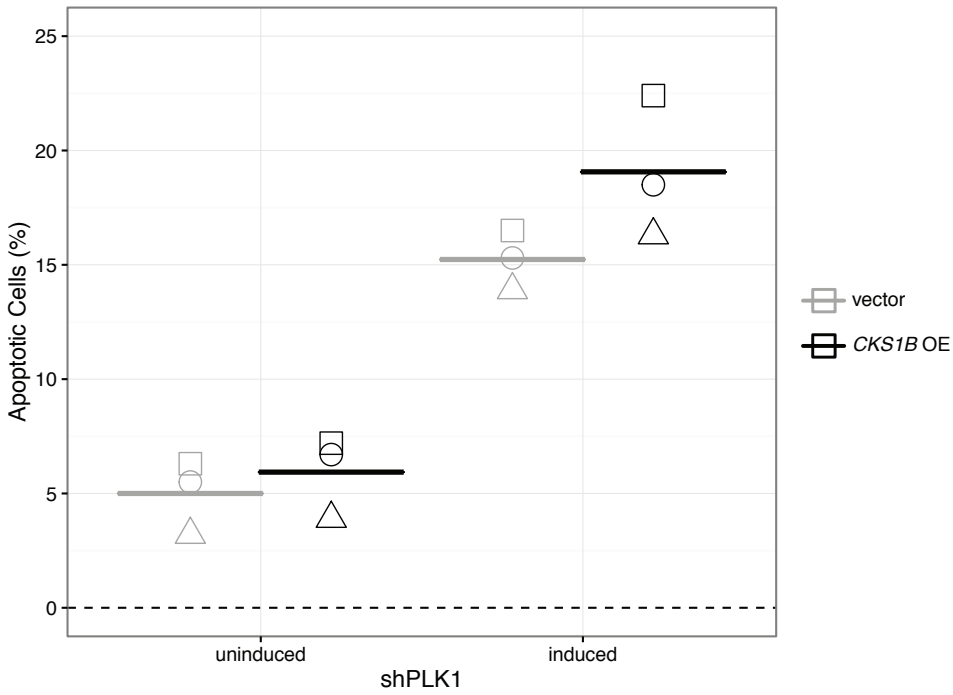
25
20
15
10
5
0
Apoptotic Cells (%)
uninduced
induced
shPLK1
vector
CKS1B OE

Figure S7

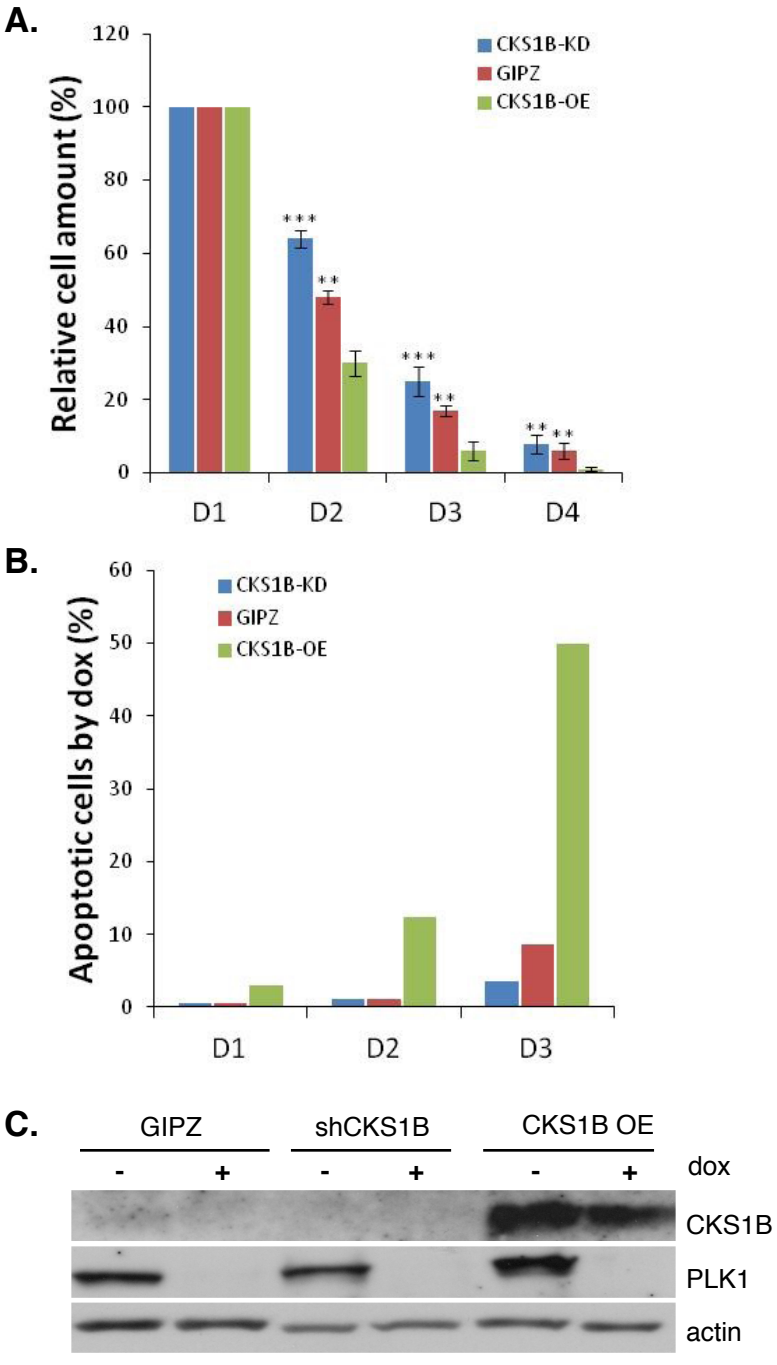
A.
Relative cell amount (%)
120
100
80
60
40
20
0
CKS1B-KD
GIPZ
CKS1B-OE
***
**
***
**
**
**
D1
D2
D3
D4
B.
Apoptotic cells by dox (%)
60
50
40
30
20
10
0
CKS1B-KD
GIPZ
CKS1B-OE
D1
D2
D3
C.
GIPZ
shCKS1B
CKS1B OE
-
+
-
+
-
+
dox
CKS1B
PLK1
actin

Table S1. Non-essential alleles isolated in independent *CKS1* SDL screens.

Function	Gene Name
Morphogenesis Checkpoint	*HSL1 HSL7*[¥] *ELM1*
PAK kinase	*CLA4*
Mitotic Exit Network	*DBF2 LTE1*[*]
Anaphase Promoting Complex	*CDH1*[*]
Cell Polarity	*VRP1*[†]
Others	*MRPS5 ANP1*

[¥] based on knockout of YBR133C (*HSL7*) in the *MAT***a** and the overlapping gene YBR134W in the *MAT*α library.

[†] based on knockout of dubious ORF YLR338W that partially overlaps verified gene *VRP1*.

[*] deletion strain was only present in *MAT***a** library and was independently verified.

Table S2. conditional alleles isolated at each temperature

Gene	23°C	27°C	30°C	33°C
AME1				*ame1-4*
ASK1				*ask1-3*
CBF2		*cbf2-1*	*cbf2-42*	*cbf2-2*
CDC10			*cdc10-4*	
CDC11		*cdc11-4*	*cdc11-1 cdc11-2 cdc11-3*	
CDC12		*cdc12-1 cdc12-td*	*cdc12-1 cdc12-td*	
CDC14		*cdc14-3*		
CDC15			*cdc15-1*	
CDC28		*cdc28-td*		
CDC3			*cdc3-1 cdc3-3*	
CDC5	*cdc5-1*	*cdc5-1*	*cdc5-1*	*cdc5-1*
DAM1			*dam1-5*	
DBF2		*dbf2-2*	*dbf2-2 dbf2-3*	*dbf2-1 dbf2-2 dbf2-3*
DPB11		*dpb11-1*		
DSN1				*dsn1-7 dsn1-8*
ERG11	*erg11-td*	*erg11-td*	*erg11-td*	*erg11-td*
LAS17	*las17-1 las17-13*	*las17-13*		
LUC7				*luc7-1*
MIF2			*mif2-3*	*mif2-3*
MYO2				*myo2-14*
NDC80			*tid3-1*	
NNF1				*nnf1-77*
NOP2				*nop2-4 nop2-6*
NSL1		*nsl1-5*		
OKP1			*okp1-5*	*okp1-5*
RPC40		*rpc40-V78R*		
RPT6			*rpt6-20*	
RSP5	*rsp5-sm1*			
SEC26				*sec26-F856AW860A*
SPC110	*spc110-220*			
SPC24		*spc24-9*	*spc24-9*	*spc24-9*
SPC25				*spc25-1*
STU1				*stu1-12 stu1-6*
SWC4			*swc4-4*	
SWD2	*swd2-ts1*	*swd2-ts1*	*swd2-ts1*	*swd2-ts1*

Gene names are listed using the standard yeast designations. Temperature conditional allele names are listed as in *Li, Z. et al. Systematic exploration of essential yeast gene function with temperature-sensitive mutants. Nat Biotechnol 29, 361–367 (2011)* and shown under each temperature condition in which they were affected by CKS1 expression in both screen datasets.

File S1. Genetic screen data for *CKS1* overexpression.

www.genetics.org/lookup/suppl/doi:10.1534/genetics.116.190231/-/DC1/FileS1.xlsx